ACS APPLIED MATERIALS & INTERFACES

Research Article

www.acsami.org

Enhanced Molecular Recognition between Nucleobases and Guanine-5′-monophosphate-disodium (GMP) by Surfactant Aggregates in Aqueous Solution

Zhang Liu,[†] Dong Wang,[‡] Meiwen Cao,[‡] Yuchun Han,[†] Hai Xu,[‡] and Yilin Wang*[,†]

[†]Key Laboratory of Colloid and Interface Science, Beijing National Laboratory for Molecular Sciences (BNLMS), Institute of Chemistry, Chinese Academy of Sciences, Beijing 100190, P. R. China

[‡]Centre for Bioengineering and Biotechnology, China University of Petroleum (East China), Qingdao 266580, P. R. China

Supporting Information

ABSTRACT: Only specific base pairs on DNA can bind with each other through hydrogen bonds, which is called the Watson−Crick (W/C) pairing rule. However, without the constraint of DNA chains, the nucleobases in bulk aqueous solution usually do not follow the W/C pairing rule anymore because of the strong competitive effect of water and the multi-interaction edges of nucleobases. The present work applied surfactant aggregates noncovalently functionalized by nucleotide to enhance the recognition between nucleobases without DNA chains in aqueous solution, and it revealed the effects of their self-assembling ability and morphologies on the recognition. The cationic ammonium monomeric, dimeric, and trimeric surfactants DTAB, 12−3−12, and 12−3−12−3−12 were chosen. The surfactants with guanine-5′-monophosphate-disodium (GMP) form micelles, vesicles, and fingerprint-like and plate-like aggregates bearing the hydrogen-bonding sites of GMP, respectively. The binding parameters of these aggregates with adenine (A), uracil (U), guanine (G), and cytosine(C) indicate that the surfactants can promote W/C recognitions in aqueous solution when they form vesicles (GMP/DTAB) or plate-like aggregates (GMP/12−3−12) with proper molecular packing compactness, which not only provide hydrophobic environments but also shield non-W/C recognition edges. However, the GMP/12−3−12 micelles with loose molecular packing, the GMP/12−3−12 fingerprint-like aggregates where the hydrogen bond sites of GMP are occupied by itself, and the GMP/12−3−12−3−12 vesicles with too strong self-assembling ability cannot promote W/C recognition. This work provides insight into how to design self-assemblies with the performance of enhanced molecule recognition.

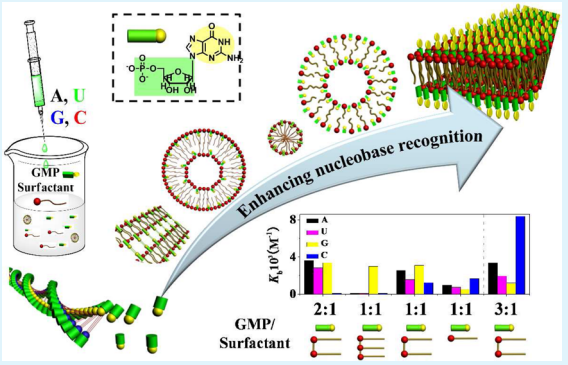

KEYWORDS: *Watson−Crick pairing, oligomeric amphiphile, self-assembling, aggregate transition, noncovalent bonds*

INTRODUCTION

Watson and Crick proposed that the two chains in deoxyribonucleic acid (DNA) are bound together through hydrogen bonds between nucleobases, and only the specific base pairs adenine(A)/thymine(T) and cytosine(C)/guanine-(G) in DNA chains can bind with each other, which is called the Watson−Crick (W/C) pairing rule.[1] So far, the W/C pairing rule has been applied in designing functional materials,[2−5] constructing artificial nanostructures,[6−8] and understanding biological functions and processes.[9−11] However, without DNA chains, W/C pairings based on hydrogen bonds are usually ineffective in aqueous solutions. This ineffectiveness is mainly caused by strong competitive binding of water to the hydrogen bonding sites on nucleobases[12,13] and the multi-interaction edges of nucleobases, including Watson−Crick, Hoogsteen/CH, and sugar edges. Various groups or sites will be available for base pairs to interact with each other depending on the edges involved.[9,14−16] To realize effective W/C recognition in aqueous solutions, aggregates and interfaces with hydrophobic environments are possible approaches to shield non-W/C edges and weaken the competiveness of water in forming hydrogen bonds with the nucleobases.

A hydrophobic environment can be constructed from three levels of dimensions: microscopic (molecules), mesoscopic (aggregate−water interfaces), and macroscopic (air−water interfaces and solid substrates).[12] The binding constant of molecularly dispersed guanidinium and phosphate in water is 1.4 M^{-1},[17] those of adenosine triphosphate (ATP) and guanidinium derivatives in micelles and vesicles are $10^2 - 10^4$ M^{-1},[18] and those of adenosine monophosphate (AMP) and ATP with a guanidinium-functionalized monolayer are 3.2×10^6 M^{-1} and 1.7×10^7 M^{-1}, respectively.[19] This means that the air−water interface and the aggregate−water interface are

Received: May 22, 2015
Accepted: June 24, 2015
Published: June 24, 2015

DOI: 10.1021/acsami.5b04441
ACS Appl. Mater. Interfaces 2015, 7, 15078−15087

Scheme 1. Chemical Structures and Abbreviations of Surfactants, Nucleotide, and Nucleobases

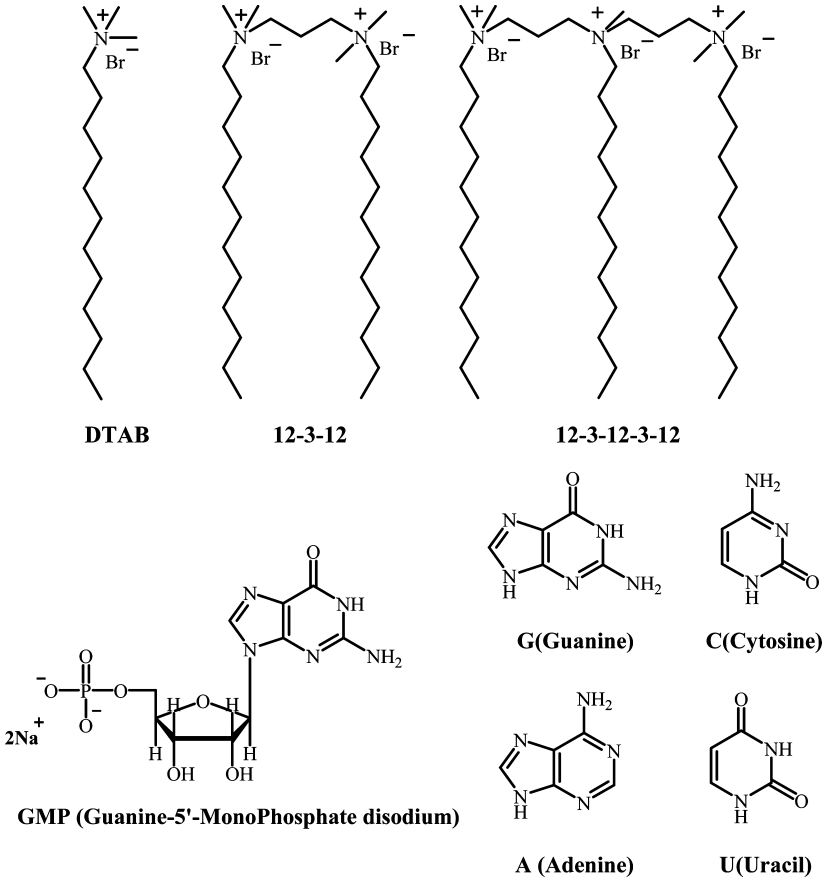

effective mediums for hydrogen bond-driven molecular recognitions.[20−27]

The aggregate−water interface has been used to enhance W/C recognition in the bulk aqueous phase.[4] The first step of obtaining an aggregate with W/C recognition ability is to fabricate a nucleotide functionalized amphiphile. The amphiphile can be formed by nucleotide and surfactant through covalent bonds or noncovalent bonds. The nucleotide functionalized amphiphiles frequently applied in bulk solution are dioleoylphosphatidyl derivatives with one nucleotide headgroup and two alkyl tails.[28−31] Berti et al.[27,32−34] synthesized a series of derivatives of adenosine, uridine, and cytidine with two alkyl tails, and they found complementary base pairings in these systems. For the nucleoside functionalized double chain surfactants, W/C pairing occurs in a vesicle with defined shape and size distribution, and the recognition process is associated with a decrease of the mean area per polar headgroup, but the aggregation number and the shape of micelles remain unchanged. Nucleotide−surfactant complexes linked by noncovalent bonds have also been studied aiming at molecular recognition. The Oda group[35] found that the solutions of cationic gemini surfactants having nucleotides as counterions show transitions to hydrogels upon addition of complementary nucleoside bases. It was also found that the nucleotides GMP and AMP form complexes with nonchiral monocationic surfactants by electrostatic interaction,[36] and guanosine, adenosine, cytidine, and uridine influence their kinetics and morphology of aggregation by cooperative effects of $\pi-\pi$ stacking, hydrophobicity, and hydrogen bonding of the bases. Among all of these interactions, W/C pairing is far from being the privileged interaction. Therefore, how to fabricate amphiphilic aggregates where W/C pairing is effective still needs to be explored.

The present work is aimed at understanding how different nucleotide-functionalized surfactant aggregates affect the W/C pairing recognition in aqueous solution. Positively charged monomeric, dimeric, and trimeric ammonium surfactants DTAB, 12−3−12, and 12−3−12−3−12 (Scheme 1) were selected because their self-assembling ability increases with increasing the amount of amphiphilic moieties. Negatively charged nucleotide guanine-5′-monophosphate-disodium (GMP) was used to form complexes with the surfactants through electrostatic attraction. It was found that the complexes of these surfactants with GMP self-assemble into spherical micelles, vesicles, and fingerprint-like and plate-like aggregates, respectively. Then the binding thermodynamic parameters of these aggregates with the nucleobases adenine (A), uracil (U), guanine (G), and cytosine (C) were determined. The results indicate that the GMP/DTAB vesicles or GMP/12−3−12 plate-like aggregates with low curvature effectively promote W/C pairing recognition in aqueous solution, while the GMP/12−3−12 micelles, GMP/12−3−12 fingerprint-like aggregates, and GMP/12−3−12−3−12 compact vesicles do not promote W/C paring recognition. The related mechanism has been revealed.

EXPERIMENTAL SECTION

Materials. Cationic ammonium gemini surfactant 12−3−12 and cationic ammonium trimeric surfactant 12−3−12−3−12 were synthesized and purified according to the corresponding literatures.[37−39] Cationic ammonium single-chain surfactant DTAB was purchased from TCI Company with a purity higher than 99.9%.

DOI: 10.1021/acsami.5b04441
ACS Appl. Mater. Interfaces 2015, 7, 15078−15087

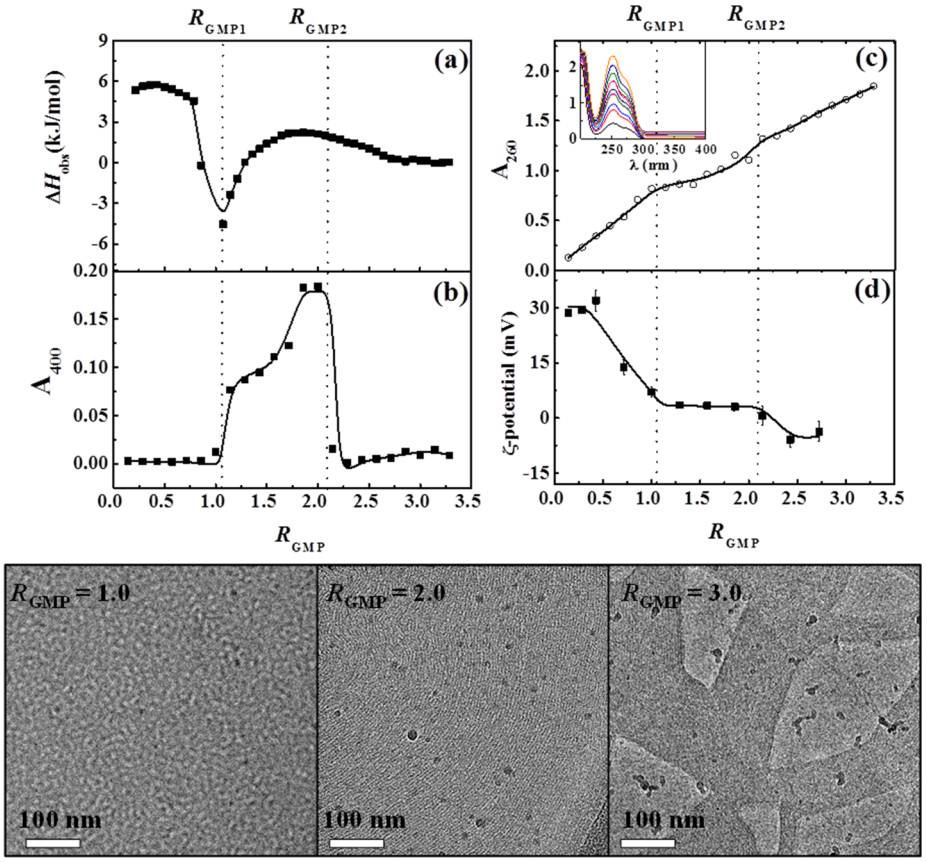

Figure 1. Variations of (a) observed enthalpy changes (ΔH_{obs}), (b) turbidity of the solution (absorbance at 400 nm), (c) characteristic absorption of GMP at 260 nm, and (d) ζ-potential plotted against the molar ratio of GMP/12−3−12 (R_{GMP}). Cryo-TEM images of the GMP/12−3−12 mixtures at 5.00 mM 12−3−12 and different R_{GMP}.

Guanine-5′-monophosphate-disodium (GMP), adenine, uracil and cytosine were purchased from Sigma Company with purity higher than 99%, and guanine was purchased from Aldrich Chemistry with purity higher than 98%. Milli-Q water (18.2 MΩ cm) was used in all experiments. The pH of all the solutions was controlled at 13.0 by NaOH for better solubility of the nucleobases.

UV−Vis Absorption. The absorption spectra were recorded in quart cuvettes (path length 0.1 mm) by a SHIMADZU UV 1601PC spectrometer. The absorbance at 400 and 260 nm were selected to monitor the solution turbidity and the characteristic absorption of nucleobases. All of the measurements were conducted at 25 ± 2 °C.

ζ-Potential and Size Measurements. The surface charge property and size distribution of the GMP/surfactant aggregates were studied by ζ-potential and dynamic light scattering (DLS) measurement at 25 °C at a scattering angle of 173° with Nano ZS (Malvern Instruments) equipped with a thermostated chamber and a 4 mW He−Ne laser (λ = 632.8 nm). Disposable capillary cells were used for ζ-potential measurements, and 12 mm square polystyrene cuvettes were used for DLS measurements.

Cryogenic Transmission Electron Microscopy (Cryo-TEM). The solutions of GMP/surfactant aggregates were embedded in a thin layer of vitreous ice on freshly carbon-coated holey TEM grids by blotting the grids with filter paper and then were plugged into liquid nitrogen. Frozen hydrated specimens were imaged by an FEI Tecnai 20 electron microscope (LaB6) operated at 200 kV in low-dose mode (about 2000 e/nm^2) and a nominal magnification of 50 000. For each specimen area, the defocus was set to 1 to 2 μm. Images were recorded on Kodak SO 163 films and then digitized by a Nikon 9000 with a scanning step of 2000 dpi corresponding to 2.54 Å/pixel.

^{1}H NMR. ^{1}H NMR spectra were recorded by a Bruker Avance 400-NMR spectrometer operating at 400 MHz at room temperature (25 ± 2 °C). Deuterium oxide (99.9%) was used to prepare the stock solutions of the surfactants and GMP. Chemical shifts were given on the parts per million scales. The center of the HDO signal (4.790 ppm) was used as the reference. In all of the ^{1}H NMR experiments, 32 scans were used and the digital resolution was 0.04 Hz/data point.

NOESY. The 2D NOESY spectra were recorded by a Bruker Avance 600-NMR spectrometer equipped with a 5 mm BBI probe operating at 600 MHz. Experiments were recorded at 25 °C by using standard pulse sequences pulprog noesyphpr in the phase sensitive mode and states-time-proportional phase incremention (States-TPPI).

Isothermal Titration Microcalorimetry (ITC). Calorimetric measurements were conducted at 25.00 ± 0.01 °C on a TAM 2277−201 microcalorimetric system (Thermometric AB, Järfälla, Sweden) with a stainless-steel sample cell of 1 mL. Each ITC curve was repeated at least twice with a deviation within ±4%. To monitor the aggregate transitions of surfactants induced by GMP, the sample cell was initially loaded with 0.6 mL surfactant solution, and then GMP solution was injected consecutively into the stirred sample cell in portions of 10 μL via a 500 μL Hamilton syringe controlled by a 612 Thermometric Lund pump until the desired concentration range had been covered. The dilution enthalpy of GMP was subtracted from the observed enthalpies. While studying the binding progress of nucleic acid bases with GMP in surfactant aggregates, the sample cell was initially loaded with 0.6 mL GMP/surfactant aggregate solution. Afterward, the solution of A, U, G or C was injected consecutively into the stirred sample cell in portions of 10 μL until the interaction progress was completed. The final dilution enthalpies of the bases were subtracted from the corresponding observed enthalpy curve of the GMP/surfactant aggregate with the bases. Finally the binding parameters of the GMP/surfactant aggregates with the bases were determined from the enthalpy curves by thermodynamic fitting.

DOI: 10.1021/acsami.5b04441
ACS Appl. Mater. Interfaces 2015, 7, 15078−15087

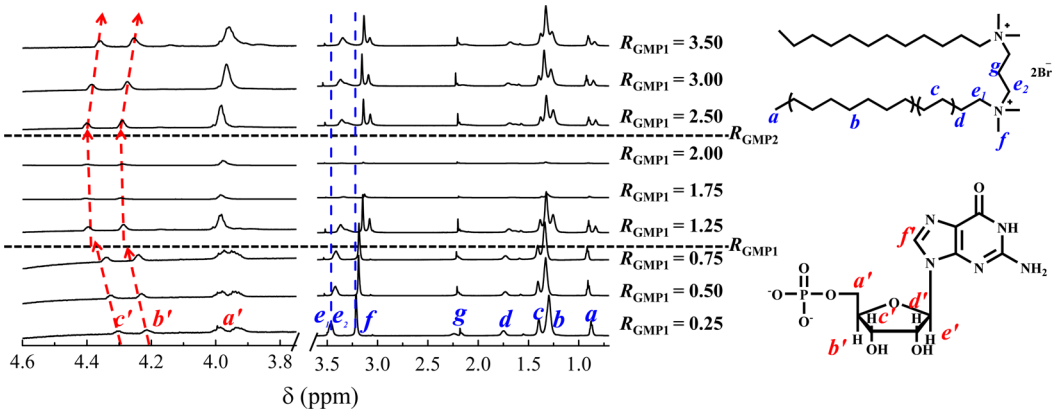

Figure 2. ^{1}H NMR spectra and proton assignments of GMP and 12−3−12 in D_2O at $C_{12-3-12}$ = 5.00 mM and different R_{GMP}.

RESULTS AND DISCUSSION

Self-assembly of 12−3−12 with GMP. By gradually mixing GMP with 12−3−12 micelles, different aggregates have been found as described below. Figure 1a presents the changes of observed enthalpy (ΔH_{obs}) against the GMP/12−3−12 molar ratio (R_{GMP}) by titrating 50.00 mM GMP solution into 5.00 mM 12−3−12 solution after the dilution enthalpy of GMP was subtracted. The corresponding changes of turbidity (absorbance at 400 nm), characteristic absorption of GMP at 260 nm, and ζ-potential are shown in Figure 1b, 1c, and 1d, respectively. 12−3−12 exists as micelles in the solutions before adding GMP because its concentration is above the CMC (1.01 mM). All of the results in Figure 1 indicate that adding GMP induces two aggregate transitions at R_{GMP1} = 1.10 and R_{GMP2} = 2.10, as marked in the figures.

When the GMP/12−3−12 molar ratio is before R_{GMP1}, electrostatic binding between oppositely charged GMP and 12−3−12 is the domain interaction. With the addition of GMP into the 12−3−12 micelles, the ΔH_{obs} values are initially between 5 and 6 kJ/mol and then sharply change from endothermic to exothermic (Figure 1a). The exothermic enthalpy is mainly contributed by the electrostatic binding between GMP and 12−3−12, while the endothermic enthalpy is mainly caused by the dehydration and the release of counterions during the electrostatic binding. The sharp change of ΔH_{obs} from endothermic to exothermic before R_{GMP1} is caused by electrostatic charge neutralization, as proved by the decrease of the ζ-potential from 30 mV to 4 mV (Figure 1d). In this region, the solution turbidity (Figure 1b) is close to zero and remains unchanged, and the characteristic absorption of GMP (Figure 1c) increases linearly, indicating that GMP has not induced an aggregate transition. The GMP/12−3−12 mixture exists as small spherical micelles, as indicated by the cryo-TEM image at R_{GMP} = 1.00 in Figure 1.

As more and more GMP molecules are bound to the 12−3−12 micelles, the aggregate transition is induced. Beyond R_{GMP1}, electrical attraction is no longer the dominant force. Figure 1a shows that exothermic enthalpy starts to decrease sharply and then turns to endothermic and almost remains constant. Meanwhile the corresponding ζ-potential (Figure 1d) decreases slightly. However, the sharp increase in turbidity (Figure 1b) reveals the formation of large aggregates. Meanwhile, the characteristic absorption of GMP (Figure 1c) no longer increases linearly with continuous addition of GMP, which indicates that the large aggregates formed have a stronger shielding effect to GMP than spherical micelles. Cryo-TEM shows that GMP/12−3−12 forms fingerprint-like aggregates in this region. When the GMP/12−3−12 molar ratio further increases beyond R_{GMP2}, the endothermic ΔH_{obs} (Figure 1a) decreases gradually to zero and then remains unchanged. Meanwhile, the turbidity (Figure 1b) also falls down to zero, the characteristic absorption of GMP (Figure 1c) increases linearly, and the ζ-potential (Figure 1d) turns to a constant negative value. In this region, GMP/12−3−12 forms plate-like aggregates, as observed under cryo-TEM.

In brief, the above results indicate that the GMP/12−3−12 mixture forms small spherical micelles, fingerprint-like aggregates, and plate-like aggregates, respectively, with the increase of the GMP/12−3−12 molar ratio. In order to better understand the base recognition of the three different aggregates conducted later, the chemical environments of the binding sites of GMP for hydrogen bonds in these aggregates are studied by NMR techniques.[40,41]

The proton assignments and ^{1}H NMR spectra of GMP and 12−3−12 are shown in Figure 2. The full ^{1}H NMR spectra are provided in the Supporting Information. The protons on 12−3−12 are assigned as *a* to *g*. The *a* and *b* protons are those on the alkyl tails in the hydrophobic core of the aggregates, *c* and *d* are in the palisade layer of the aggregates, and e_1, e_2, *f*, and *g* are near the headgroups at the aggregate−solution interface. The protons on GMP are assigned as *a*′ to *f*′ from the hydrophilic end to the hydrophobic end. The variations of the frequency, intensity, and shape of the peaks in the ^{1}H NMR spectra reflect the differences of the electrical environments and the steric configurations of GMP and 12−3−12 in the three kinds of aggregates. Below R_{GMP1}, GMP electrostatically binds with 12−3−12 in small spherical micelles. The protons on the headgroups of 12−3−12 (e_1, e_2, and *f*) upfield shift while the protons on GMP (*b*′ and *c*′) downfield shift. This indicates that with the binding of GMP to 12−3−12 in micelles, the electron density of GMP decreases, while that of 12−3−12 increases. Beyond R_{GMP1}, the micelles transform to the fingerprint-like aggregates. Between R_{GMP1} and R_{GMP2}, the chemical shift of the protons on both GMP and 12−3−12 almost remains unchanged, while the signal intensity decreases seriously. The decrease of the signal intensity results from the existence of the large fingerprint-like aggregates. Beyond R_{GMP2}, the *b*′ and *c*′ protons on GMP in the plate-like aggregates shift upfield, where the aggregates carry negative charges and the protons experience more electron density. In particular, the 12−3−12 protons on the hydrophobic tail (*a* and *b*) and the methyl groups (*f*) at the headgroups split into two peaks in the

DOI: 10.1021/acsami.5b04441
ACS Appl. Mater. Interfaces 2015, 7, 15078−15087

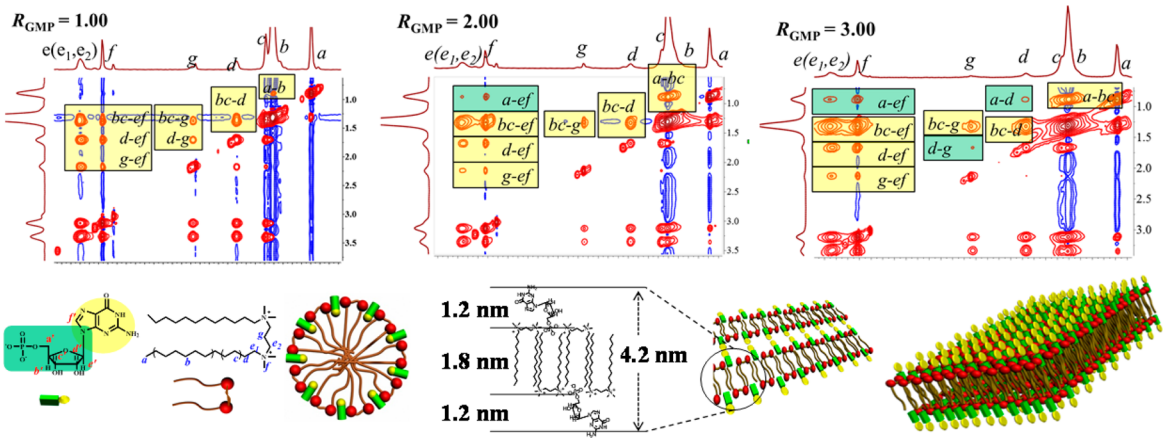

Figure 3. NOE spectra of the GMP/12−3−12 mixtures at 5.00 mM 12−3−12 and R_{GMP} = 1.00, 2.00, and 3.00 in D_2O. The chemical structures under the NOE spectra show the molecule arrangement of GMP and 12−3−12 in the fingerprint-like and plate-like aggregates. The possible models of micelles and fingerprint-like and plate-like aggregates are presented.

fingerprint-like and plate-like aggregates. This means that the protons (*a*, *b*, and *f*) are in two different electronic environments and their motions are greatly limited. Meanwhile the two narrow peaks of *a′* on GMP merge into one broad peak. The disappearance of the fine structure means that GMP enters a more polar environment, which suggests that GMP may be located in the palisade layer of the micelles but may exist at the aggregate−water interface in the fingerprint-like and plate-like aggregates.

In order to know the molecule packing situation of GMP and 12−3−12, the NOE technique is used. Normally cross peaks are observed in the NOE spectra when the distance between two protons is less than 5 Å.[42] The NOE spectra of the GMP/12−3−12 mixtures at R_{GMP} = 1.00, 2.00, and 3.00 are shown in Figure 3, corresponding to the situations of micelles, fingerprint-like aggregates, and plate-like aggregates, respectively. As the peaks of e_1 and e_2 can be hardly separated from each other, *e* is used to represent the two protons in the NOE spectra. The cross peaks in the yellow regions appear in these three kinds of aggregates, reflecting the interactions of *a-b*, *a-bc*, *bc-dg*, and *bcdg-ef*. The cross peaks of *a-b* and *a-bc* indicate the intermolecular overlap packing of the alkyl tails, while the cross peaks of *bc-dg* and *bcdg-ef* mean that the 12−3−12 molecules are packed in a very compressed way. Comparing the NOE spectra at R_{GMP} = 1.00 (micelle) with those at R_{GMP} = 2.00 (fingerprint-like aggregate) and R_{GMP} = 3.00 (plate-like aggregate), the main differences appear in the green regions. The fingerprint-like and plate-like aggregates have cross peaks between *a* and *ef*, but the micelles do not, indicating that the protons at the terminal of alkyl chains (*a*) are close in space with the headgroup (*e* and *f*) in the fingerprint-like and plate-like aggregates. This implies that the 12−3−12 molecules in the fingerprint-like and plate-like aggregates are deeply overlapped head by tail and form a double layer structure. In addition, the fingerprint-like and plate-like aggregates have no cross peaks between *a* and *g*, which means that the hydrophobic tails in the double layer are arranged side by side. Moreover, the plate-like aggregates have cross peaks in the proton pairs of *d*−*g* or *a*−*d*, which means that the surfactant molecules are more compactly packed in the plate-like aggregates than in the fingerprint-like aggregates. The thickness of the double layer structure calculated from the molecular structures is 4.2 nm, consisting of the fingerprint interval observed in the cryo-TEM image in Figure 1.

Self-assembly of DTAB with GMP. Compared with gemini surfactant 12−3−12, its corresponding monomeric surfactant DTAB shows weaker aggregation ability and larger CMC (14.80 mM). Similar to the GMP/12−3−12 system, the aggregate transition of DTAB micelles induced by GMP has also been studied. Figure 4a presents the change of ΔH_{obs}

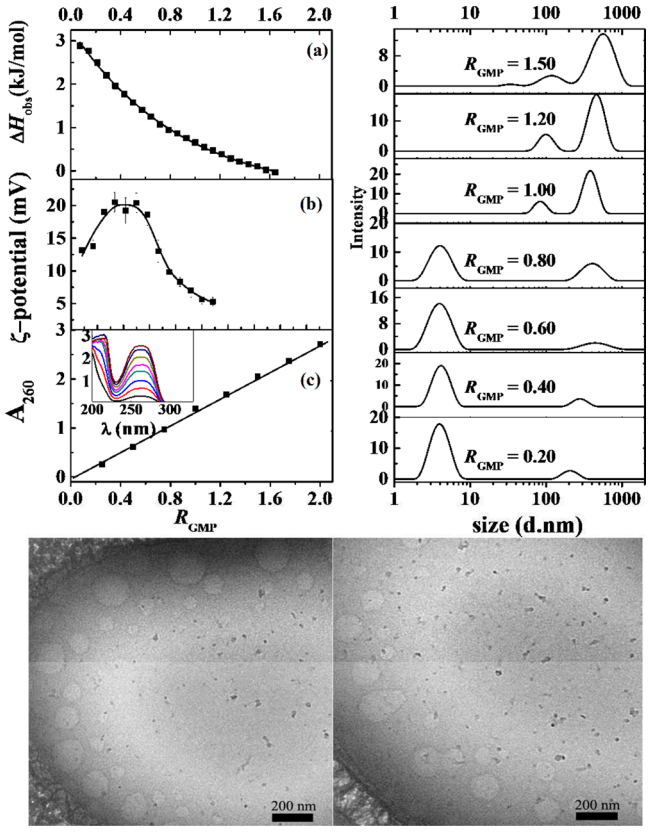

Figure 4. Variations of (a) observed enthalpy changes (ΔH_{obs}), (b) ζ-potential, and (c) characteristic absorption of GMP and size distribution (hydrodynamic diameter) at 20.00 mM DTAB solution and different R_{GMP}. Cryo-TEM images of GMP/DTAB mixed solution at R_{GMP} = 1.00 and 20.00 mM DTAB.

DOI: 10.1021/acsami.5b04441
ACS Appl. Mater. Interfaces 2015, 7, 15078−15087

against the GMP/DTAB molar ratio (R_{GMP}) by titrating 100.00 mM GMP into 20.00 mM DTAB solution. With the addition of GMP, the endothermic enthalpy decreases from 3 to 0 kJ/mol gradually and shows no obvious turning point. Meanwhile, the ζ-potential (Figure 4b) increases from 13 to 20 mV, and then the ζ-potential decreases gradually to 5 mV when the GMP/DTAB molar ratio increases to 1.00. In the whole process, the characteristic absorption of GMP (Figure 4c) increases linearly, indicating the consistent binding process of GMP with DTAB. The DLS size measurement indicates that small micelles of ~4 nm are the main aggregates at lower R_{GMP}; however, when R_{GMP} is larger than 1.00, small micelles disappear, but larger aggregates of hundreds of nanometers coexist. The larger aggregates are vesicles, as proved by the cryo-TEM image in Figure 4. Therefore, the addition of GMP into DTAB micelles causes the transition from small micelles to larger vesicles. The GMP/DTAB vesicles are also chosen to conduct the base recognition study described in the later section.

To understand the structural details of the GMP/DTAB vesicles, the NOE spectrum of the GMP/DTAB mixture is shown in Figure 5. The cross peak of GMP and DTAB between

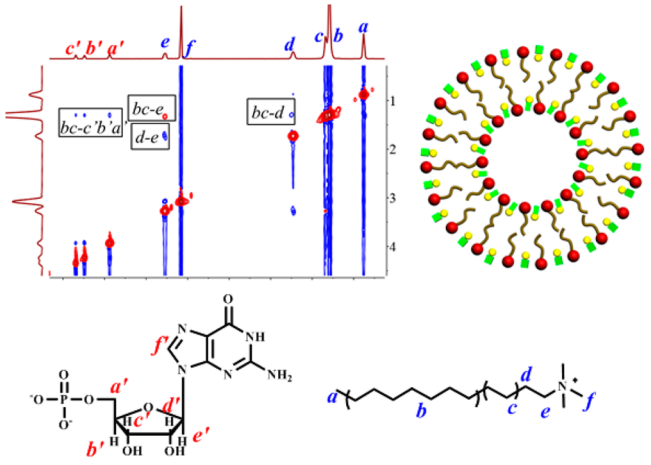

Figure 5. NOE spectrum of the GMP/DTAB mixtures at R_{GMP} = 1.00 and C_{DTAB} = 20.00 mM in D_2O, and the possible model of the mixed vesicle and proton assignments of GMP and DTAB.

bc and *a′b′c′*, indicates that GMP is inserted into the double layer of the mixed vesicles. Moreover, cross peaks appear in the proton pairs of *bc-e*, *bc-d*, and *d-e*, but there are no cross peaks between *a* and other protons, which means that the double layer is arranged head by head and tail by tail as shown in the cartoon of Figure 5. The molecular packing is quite different from the GMP/12−3−12 aggregates shown in Figure 3.

Self-assembly of 12−3−12−3−12 with GMP. In the three surfactants selected, 12−3−12−3−12 has the strongest self-assembling ability and the smallest CMC (0.16 mM).[37] The aggregate transition of the 12−3−12−3−12 micelles induced by adding GMP has also been studied. Figure 6 indicates that aggregate transition occurs when the GMP/12−3−12−3−12 molar ratio R_{GMP} increases to 0.50. When R_{GMP} is below 0.50, the observed enthalpy ΔH_{obs} (Figure 6a) turns from zero to exothermic and continuously increases until it reaches a maximum. Beyond 0.50, the exothermic ΔH_{obs} becomes smaller, then turns into an endothermic value, and finally returns to zero. In this process, the size of the aggregates increases from around 10 nm before R_{GMP} = 0.50 to hundreds of nanometers beyond R_{GMP} = 0.50. The smaller aggregates are

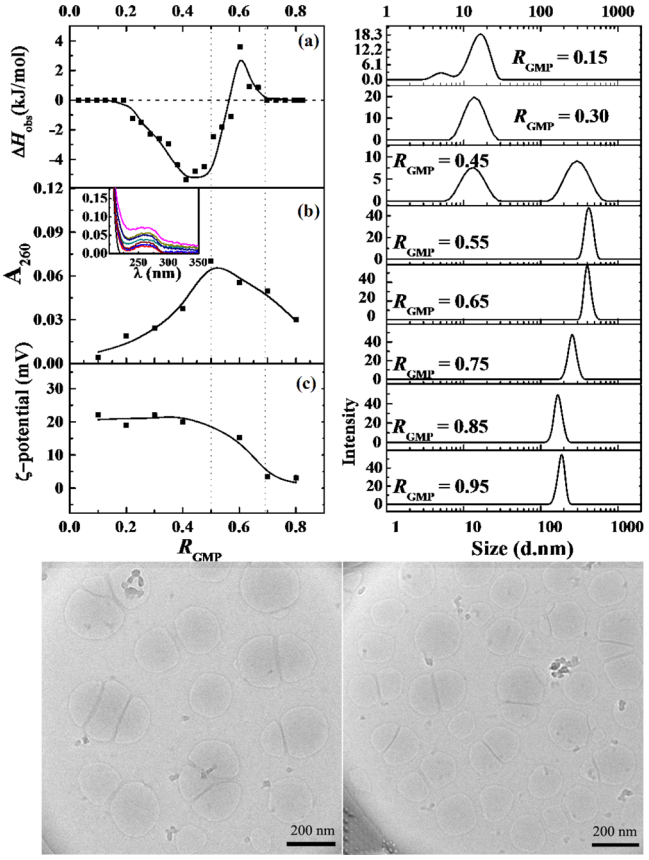

Figure 6. Variations of (a) observed enthalpy changes (ΔH_{obs}) against GMP/12−3−12−3−12 molar ratio (R_{GMP}) in the process of titrating 5.00 mM GMP into 1.00 mM 12−3−12−3−12 at 25.00 °C, (b) characteristic absorption of GMP at 260 nm, (c) ζ-potential and the size distribution of hydrodynamic diameter at different R_{GMP} values. Cryo-TEM image of the GMP/12−3−12−3−12 mixture at R_{GMP} = 1.00 and 1.00 mM 12−3−12−3−12.

small micelles while the larger aggregates are vesicles, as proved by the cryo-TEM images (Figure 6). Meanwhile, the ζ-potential remains stable at 20 mV and the characteristic absorption of GMP (A_{260}) increases. Beyond R_{GMP} = 0.50, the ζ-potential reduces to around zero and the characteristic absorption of GMP decreases almost linearly. These variations indicate that the electrostatic binding of anionic GMP with cationic 12−3−12−3−12 leads the micelles to form nearly charge-neutralized vesicles, which holds great electronic shielding ability. Besides, the decrease of the vesicle size from DLS beyond R_{GMP} = 0.50 and the cryo-TEM image show that the larger vesicles tend to separate into smaller vesicles with the further addition of GMP. This may result from the inserting of GMP into the double layers of 12−3−12−3−12.

The NOE spectrum of the GMP/12−3−12−3−12 vesicle has also been obtained, but the signal intensity is very weak and the cross peaks are lost in noise, which results from the formation of large and compact vesicles with great shielding ability.

Influence of Surfactant Aggregates on W/C Base Pair Recognition. On the basis of the above studies, we study the performance of the GMP/12−3−12 micelle, GMP/12−3−12 fingerprint-like aggregate, GMP/12−3−12 plate-like aggregate, GMP/DTAB vesicle, and GMP/12−3−12−3−12 vesicle in base pair recognition by using ITC. Figure 7 presents the variation of ΔH_{obs} against the nucleobase/surfactant molar

DOI: 10.1021/acsami.5b04441
ACS Appl. Mater. Interfaces 2015, 7, 15078−15087

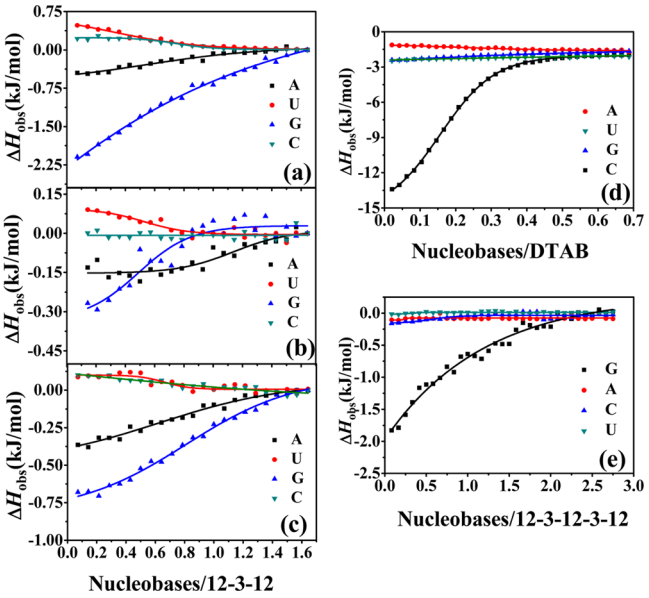

Figure 7. Observed enthalpy changes ΔH_{obs} by titrating A, U, G, or C into the GMP/12−3−12 micelles (a, R_{GMP} = 1.00), the fingerprint-like aggregates (b, R_{GMP} = 2.00), the plate-like aggregates (c, R_{GMP} = 3.00), the GMP/DTAB vesicles (d, R_{GMP} = 1.00), and the GMP/12−3−12−3−12 vesicles (e, R_{GMP} = 1.00 and $C_{12-3-12-3-12}$ = 1.00 mM).

ratios in the process of separately titrating the nucleobase solution of A, U, G, or C into the aqueous solution of the GMP/surfactant aggregate solutions above. The ITC curves are approximately sigmoidal in shape and change from endothermic or exothermic values to zero, reaching the saturation point of binding. The ΔH_{obs} curves for titrating the nucleobases into the surfactant solutions without GMP and into the GMP solution without surfactants were carried out separately. The enthalpy changes of the corresponding processes are very small compared with the enthalpy changes for titrating the nucleobases into the GMP/surfactant solutions. This suggests that the enthalpy changes of titrating the nucleobases into the GMP/surfactant solutions are mainly contributed by the binding of the nucleobases with GMP in the GMP/surfactant aggregates. Before fitting the ITC binding curves of nucleobases being titrated into the GMP/surfactant solution, the corresponding titrating curve for each kind of nucleobase being titrated into the surfactant solution has been deducted.

These ITC curves are analyzed with the thermodynamic method described in the Supporting Information. The binding constant (K_b), the number of binding sites (N), and the binding enthalpy (ΔH_b) of the bases with GMP in different GMP/surfactant aggregates are obtained. The Gibbs free energy (ΔG_b) is calculated from $\Delta G_b = -RT \ln K_b$, and the entropy change (ΔS_b) is calculated from $\Delta S_b = (\Delta H_b - \Delta G_b)/T$. The derived interaction thermodynamic parameters are listed in Table 1. For a more clear comparison, ΔH_{obs} and K_b of the bases binding with GMP in the aggregates are summarized in Figure 8.

Very interestingly, the binding constants K_b of A, U, G, and C with the GMP/12−3−12 (3:1) plate-like aggregates and the GMP/DTAB (1:1) vesicles indicate that base C exhibits the strongest binding ability with GMP; that is, the binding constants of C with GMP in these two aggregates are at least two times higher than those of A, U, and G with GMP in these aggregates. The results indicate that effective W/C recognition is realized in the GMP/12−3−12 plate-like aggregates and the GMP/DTAB vesicles. But in the GMP/12−3−12 (1:1) micelles, and the GMP/12−3−12 (2:1) fingerprint-like aggregates, and the GMP/12−3−12−3−12 (1:1) vesicles, the binding constants of C with GMP are much lower than those of A, U, and G with GMP. The binding of C with GMP is nearly undetectable even in the GMP/12−3−12 fingerprint-like aggregates and the GMP/12−3−12−3−12 vesicles,. In brief, W/C base pair recognition in aqueous solution is greatly enhanced by the GMP/12−3−12 plate-like aggregates and the GMP/DTAB vesicles, but the W/C base pair recognition is ineffective for the other aggregates.

The obvious differences among the binding abilities of the A, U, G, and C with different aggregates rely on different molecule

Table 1. Thermodynamic Parameters of the Bases Binding to Different Surfactant Aggregates Derived from ITC Curves

GMP/Surfactant Aggregates	Bases	N	ΔH_b (kJ/mol)	$T\Delta S_b$ (kJ/mol)	ΔG_b (kJ/mol)	K_b (10^3 M^{-1})
GMP/12−3−12 = 1.00 Micelles	A	0.89	−0.18	19.21	−19.39	2.53
	U	0.98	0.13	18.34	−18.20	1.58
	G	0.97	−0.34	19.59	−19.92	3.12
	C	0.74	0.10	19.46	−19.36	2.49
GMP/12−3−12 = 2.00 Fingerprint-like aggregates	A	0.57	−0.074	20.21	−20.28	3.61
	U	0.33	0.055	19.71	−19.66	2.85
	G	0.30	−0.19	19.96	−20.15	3.38
	C					
GMP/12−3−12 = 3.00 Plate-like aggregates	A	0.26	−0.23	19.96	−20.19	3.39
	U	0.20	0.29	19.09	−18.82	1.95
	G	0.28	−1.13	16.59	−17.72	1.22
	C	0.27	0.12	22.45	−22.34	8.04
GMP/DTAB = 1.00 Vesicles	A	0.39	0.21	17.21	−17.00	0.98
	U	0.26	−0.14	16.34	−16.48	0.77
	G	0.46	−0.38	15.22	−15.59	0.53
	C	0.22	−5.15	13.47	−18.62	1.69
GMP/12−3−12−3−12 = 1.00 Vesicles	A					
	U					
	G	1.11	−4.48	15.59	−20.08	2.99
	C					

DOI: 10.1021/acsami.5b04441
ACS Appl. Mater. Interfaces 2015, 7, 15078−15087

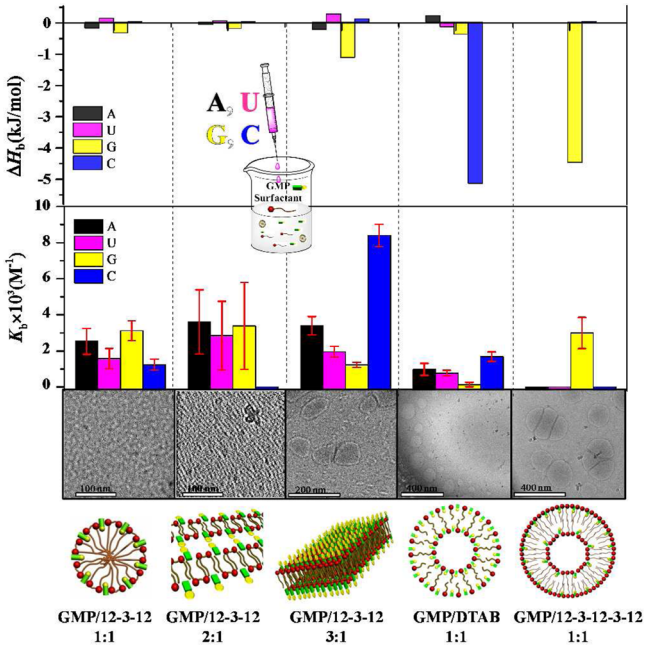

Figure 8. ΔH_b and K_b of nucleobases binding to different GMP/surfactant aggregates.

arrangements of GMP and surfactant packing situations in the surfactant aggregates, which have been verified by the above ^{1}H NMR and NOE experiments.

In the GMP/12−3−12 micelles, the nucleobase part of GMP (yellow part of GMP in Figure 3) has plugged into the palisade layer of the micelles. The hydrophobic environments of the micelles weaken the competitiveness of water molecules in forming hydrogen bonds with nucleobases, which enhances the binding of all the nucleobases to GMP. However, as the micelle/solution interface is relatively loose, GMP is rather rotatable and can interact with nucleobases from both W/C recognition edges and non-W/C recognition edges. This is the reason why the binding constants of A, U, G, and C with GMP show no obvious differences in micelles.

In the GMP/12−3−12 fingerprint-like aggregates, GMP stays at the fingerprint clearance; thus, its phosphate part directs to the headgroup of 12−3−12, and its nucleobase parts remain directed toward each other and form hydrogen bonds. In these fingerprint-like aggregates, the binding enthalpies of A, U, G, and C with GMP are quite small compared with other systems and the errors of K_b are remarkable (Figure 8), indicating that the interaction between nucleobases and GMP is quite weak. This possible reason is that the hydrogen binding sites on GMP have been occupied when forming the fingerprint-like aggregates.

In the GMP/12−3−12 plate-like aggregates, the phosphate part of GMP is anchoring at the aggregate interface and the base part stays toward the bulk solution. Even though the GMP has not plugged into the hydrophobic environment, the K_b value of the complementary nucleobase C with GMP is much larger than that of other noncomplementary nucleobases (A, U, and G), leading to the enhancement of W/C recognition. The plate-like aggregates limit the movement of GMP and shield some of the binding edges of GMP. Just like the DNA chains which hold tightly one-dimensional binding sites of bases, this plate-like aggregate concentrates two-dimensional binding sites of GMP at the aggregate/water interface. These factors significantly enhance the W/C recognition ability of GMP in the surfactant aggregates.

In particular, although both GMP/DTAB and GMP/12−3−12−3−12 mixtures form vesicles, their recognition performances are quite different. In the vesicles, the recognition sites of GMP are buried in the palisade layer. Because the GMP and surfactant molecules are packed more tightly in vesicles than in micelles, the vesicles prefer W/C base pairs. That is why effective W/C recognition is realized in the GMP/DTAB vesicles. However, for the GMP/12−3−12−3−12 vesicles, GMP is inserted into too tightly packed molecules of trimeric 12−3−12−3−12 due to its strong self-assembling ability, so the A, U, and C except G can hardly plug into the hydrophobic layer of the vesicles and bind with GMP. Since the structure of base G is the same as the nucleobase part of GMP, the same configuration may allow G to reach the nucleobase part of GMP and bind with it. Thus, the W/C recognition is ineffective in the case of the GMP/12−3−12−3−12 vesicles.

In summary, the surfactant self-assemblies can be conveniently used to mimic the restriction effect of DNA chains on nucleobases, which makes the molecular recognition effective. By adjusting the morphologies of surfactant aggregates and the molecular packing of bases and surfactants, effective W/C recognition can be achieved and enhanced.

CONCLUSION

The effects of the surfactant self-assembling ability and aggregate structures on the enhancement of W/C recognition in aqueous solution have been studied. The cationic ammonium monomeric, dimeric, and trimeric surfactants DTAB, 12−3−12, and 12−3−12−3−12 were chosen, and their aggregation properties in the presence of GMP have been studied by ITC, ζ-potential, UV−visual spectroscopy, DLS, and cryo-TEM. ^{1}H NMR and NOE techniques have been used to investigate the molecular interactions and spatial positions of surfactants and GMP in the aggregates. Micelles, vesicles, and fingerprint-like and plate-like aggregates bearing the hydrogen-bonding sites of GMP were constructed, and their binding parameters with nucleobases A, U, G, and C were determined by ITC. It is found that the W/C pairing rule is effective in GMP/DTAB vesicles and GMP/12−3−12 plate-like aggregates. The former one is effective because the recognition sites are buried in a hydrophobic environment, while the latter one is because an abundance of recognition sites of GMP are available on the plate-like aggregates interface and the aggregates limit the movement of GMP. The GMP/12−3−12 micelles fail to shield non-W/C recognition edges of GMP, resulting in the formation of non-W/C base pairs. In the long GMP/12−3−12 fingerprint-like aggregates, GMP forms hydrogen bonds between themselves and fails to recognize other nucleobases. In the GMP/12−3−12−3−12 vesicles, GMP and 12−3−12−3−12 molecules are so tightly packed that other nucleobases can hardly plug into the hydrophobic layer to bind with GMP except G. Obviously, if W/C base recognition in aqueous solution is enhanced strongly depends on the aggregate structure and the molecular packing of GMP and surfactants inside. The nucleotide/surfactant complexes with great self-assembling abilities can assemble into stable structures through hydrogen bond and hydrophobic interaction. The proper surfactant aggregates can effectively limit the movement of GMP and shield non-W/C pair edges. Once the hydrogen bonding sites on nucleobases have been occupied, the aggregates no longer exhibit recognition ability. In addition,

DOI: 10.1021/acsami.5b04441
ACS Appl. Mater. Interfaces 2015, 7, 15078−15087

surfactants with superior assembling abilities do not always show better performance in enhancing base recognition. By adjusting the hydrophobic and electrostatic interactions of noncovalently linked nucleotide−surfactant complexes, the self-assembling ability and aggregate structure can be optimized to enhance W/C base recognition ability. This work provides new insight into how to design self-assemblies with the performance of enhanced molecular recognition.

■ ASSOCIATED CONTENT

Supporting Information

ITC analysis process and ^{1}H NMR spectra of GMP/12−3−12. Descriptions about syntheses, purification, and ^{1}H NMR, MS-ESI, and elemental analyses of 12−3−12 and 12−3−12−3−12. The Supporting Information is available free of charge on the ACS Publications website at DOI: 10.1021/acsami.5b04441.

■ AUTHOR INFORMATION

Corresponding Author

* E-mail: yilinwang@iccas.ac.cn.

Notes

The authors declare no competing financial interest.

■ ACKNOWLEDGMENTS

This work was supported by the Chinese Academy of Sciences and National Natural Science Foundation of China (21025313, 21321063)

■ REFERENCES

(1) Crick, F.; Watson, J. Molecular Structure of Nucleic Acids: A Structure for Deoxyribose Nucleic Acid. *Nature* **1953**, *171*, 737−738.
(2) Seeman, N. C. DNA in a Material World. *Nature* **2003**, *421*, 427−431.
(3) Ding, B.; Sha, R.; Seeman, N. C. Pseudohexagonal 2D DNA Crystals from Double Crossover Cohesion. *J. Am. Chem. Soc.* **2004**, *126*, 10230−10231.
(4) Rosemeyer, H. Nucleolipids: Natural Occurrence, Synthesis, Molecular Recognition, and Supramolecular Assemblies as Potential Precursors of Life and Bioorganic Materials. *Chem. Biodiversity* **2005**, *2*, 977−1063.
(5) Allain, V.; Bourgaux, C.; Couvreur, P. Self-Assembled Nucleolipids: From Supramolecular Structure to Soft Nucleic Acid and Drug Delivery Devices. *Nucleic Acids Res.* **2012**, *40*, 1891−1903.
(6) Mamdouh, W.; Dong, M.; Xu, S.; Rauls, E.; Besenbacher, F. Supramolecular Nanopatterns Self-Assembled by Adenine−Thymine Quartets at the Liquid/Solid Interface. *J. Am. Chem. Soc.* **2006**, *128*, 13305−13311.
(7) Mao, C.; LaBean, T. H.; Reif, J. H.; Seeman, N. C. Logical Computation Using Algorithmic Self−Assembly of DNA Triple−Crossover Molecules. *Nature* **2000**, *407*, 493−496.
(8) Yan, H.; Park, S. H.; Finkelstein, G.; Reif, J. H.; LaBean, T. H. DNA-Templated Self-Assembly of Protein Arrays and Highly Conductive Nanowires. *Science* **2003**, *301*, 1882−1884.
(9) Leontis, N. B.; Stombaugh, J.; Westhof, E. The Non-Watson-Crick Base Pairs and Their Associated Isostericity Matrices. *Nucleic Acids Res.* **2002**, *30*, 3497−3531.
(10) Moran, S.; Ren, R. X.-F.; Kool, E. T. P. A Thymidine Triphosphate Shape Analog Lacking Watson−Crick Pairing Ability Is Replicated with High Sequence Selectivity. *Proc. Natl. Acad. Sci. U. S. A.* **1997**, *94*, 10506−10511.
(11) Wolfle, W. T.; Washington, M. T.; Kool, E. T.; Spratt, T. E.; Helquist, S. A.; Prakash, L.; Prakash, S. Evidence for a Watson−Crick Hydrogen Bonding Requirement in DNA Synthesis by Human DNA Polymerase κ. *Mol. Cell. Biol.* **2005**, *25*, 7137−7143.
(12) Ariga, K.; Kunitake, T. Molecular Recognition at Air−Water and Related Interfaces: Complementary Hydrogen Bonding and Multisite Interaction. *Acc. Chem. Res.* **1998**, *31*, 371−378.
(13) Kneeland, D. M.; Ariga, K.; Lynch, V. M.; Huang, C. Y.; Anslyn, E. V. Bis(Alkylguanidinium) Receptors for Phosphodiesters: Effect of Counterions, Solvent Mixtures, and Cavity Flexibility on Complexation. *J. Am. Chem. Soc.* **1993**, *115*, 10042−10055.
(14) Shankar, A.; Jagota, A.; Mittal, J. DNA Base Dimers Are Stabilized by Hydrogen−Bonding Interactions Including Non-Watson−Crick Pairing near Graphite Surfaces. *J. Phys. Chem. B* **2012**, *116*, 12088−12094.
(15) Williams, D. H.; Cox, J. P. L.; Doig, A. J.; Gardner, M.; Gerhard, U.; Kaye, P. T.; Lal, A. R.; Nicholls, I. A.; Salter, C. J.; Mitchell, R. C. Toward the Semiquantitative Estimation of Binding Constants. Guides for Peptide−Peptide Binding in Aqueous Solution. *J. Am. Chem. Soc.* **1991**, *113*, 7020−7030.
(16) Quigley, G.; Ughetto, G.; van der Marel, G.; van Boom, J.; Wang, A.; Rich, A. Non-Watson−Crick G.C and A.T Base Pairs in a DNA−Antibiotic Complex. *Science* **1986**, *232*, 1255−1258.
(17) Springs, B.; Haake, P. Equilibrium Constants for Association of Guanidinium and Ammonium Ions with Oxyanions: The Effect of Changing Basicity of the Oxyanion. *Bioorg. Chem.* **1977**, *6*, 181−190.
(18) Onda, M.; Yoshihara, K.; Koyano, H.; Ariga, K.; Kunitake, T. Molecular Recognition of Nucleotides by the Guanidinium Unit at the Surface of Aqueous Micelles and Bilayers. A Comparison of Microscopic and Macroscopic Interfaces. *J. Am. Chem. Soc.* **1996**, *118*, 8524−8530.
(19) Sasaki, D. Y.; Kurihara, K.; Kunitake, T. Multiple-Point Binding of Atp and Amp to a Guanidinium−Functionalized Monolayer. *J. Am. Chem. Soc.* **1991**, *113*, 9685−9686.
(20) Nowick, J. S.; Cao, T.; Noronha, G. Molecular Recognition between Uncharged Molecules in Aqueous Micelles. *J. Am. Chem. Soc.* **1994**, *116*, 3285−3289.
(21) Bonar-Law, R. P. Recognition by a Solubilized Receptor: Hydrogen Bonding, Solvophobic Interactions, and Solvent Engineering inside Micelles. *J. Am. Chem. Soc.* **1995**, *117*, 12397−12407.
(22) Miao, W.; Du, X.; Liang, Y. Molecular Recognition of Nucleolipid Monolayers of 1-(2-Octadecyloxycarbonylethyl) Cytosine to Guanosine at the Air−Water Interface and Langmuir−Blodgett Films. *Langmuir* **2003**, *19*, 5389−5396.
(23) Miao, W.; Du, X.; Liang, Y. Molecular Recognition of 1-(2-Octadecyloxycarbonylethyl)Cytosine Monolayers to Guanosine at the Air−Water Interface Investigated by Infrared Reflection−Absorption Spectroscopy. *J. Phys. Chem. B* **2003**, *107*, 13636−13642.
(24) Wang, Y.; Du, X.; Miao, W.; Liang, Y. Molecular Recognition of Cytosine- and Guanine-Functionalized Nucleolipids in the Mixed Monolayers at the Air−Water Interface and Langmuir−Blodgett Films. *J. Phys. Chem. B* **2006**, *110*, 4914−4923.
(25) Xin, Y.; Kong, X.; Zhang, X.; Lv, Z.; Du, X. Self-Assembly and Molecular Recognition of Adenine- and Thymine-Functionalized Nucleolipids in the Mixed Monolayers and Thymine-Functionalized Nucleolipids on Aqueous Melamine at the Air−Water Interface. *Langmuir* **2012**, *28*, 11153−11163.
(26) Kurihara, K.; Ohto, K.; Honda, Y.; Kunitake, T. Efficient, Complementary Binding of Nucleic Acid Bases to Diaminotriazine-Functionalized Monolayers on Water. *J. Am. Chem. Soc.* **1991**, *113*, 5077−5079.
(27) Berti, D.; Franchi, L.; Baglioni, P.; Luisi, P. L. Molecular Recognition in Monolayers. Complementary Base Pairing in Dioleoylphosphatidyl Derivatives of Adenosine, Uridine, and Cytidine. *Langmuir* **1997**, *13*, 3438−3444.
(28) Bombelli, F. B.; Berti, D.; Almgren, M.; Karlsson, G.; Baglioni, P. Light Scattering and Cryo-Transmission Electron Microscopy Investigation of the Self-Assembling Behavior of Di−C12p−Nucleosides in Solution. *J. Phys. Chem. B* **2006**, *110*, 17627−17637.
(29) Bonaccio, S.; Capitani, D.; Segre, A. L.; Walde, P.; Luisi, P. L. Liposomes from Phosphatidyl Nucleosides: An NMR Investigation. *Langmuir* **1997**, *13*, 1952−1956.

DOI: 10.1021/acsami.5b04441
ACS Appl. Mater. Interfaces 2015, 7, 15078−15087

(30) Berndt, P.; Kurihara, K.; Kunitake, T. Measurement of Forces between Surfaces Composed of Two−Dimensionally Organized, Complementary and Noncomplementary Nucleobases. *Langmuir* **1995**, *11*, 3083−3091.
(31) Gissot, A.; Camplo, M.; Grinstaff, M. W.; Barthelemy, P. Nucleoside, Nucleotide and Oligonucleotide Based Amphiphiles: A Successful Marriage of Nucleic Acids with Lipids. *Org. Biomol. Chem.* **2008**, *6*, 1324−1333.
(32) Berti, D.; Baglioni, P.; Bonaccio, S.; Barsacchi-Bo, G.; Luisi, P. L. Base Complementarity and Nucleoside Recognition in Phosphatidylnucleoside Vesicles. *J. Phys. Chem. B* **1998**, *102*, 303−308.
(33) Murgia, S.; Lampis, S.; Angius, R.; Berti, D.; Monduzzi, M. Orientation and Specific Interactions of Nucleotides and Nucleolipids inside Monoolein−Based Liquid Crystals. *J. Phys. Chem. B* **2009**, *113*, 9205−9215.
(34) Berti, D.; Luisi, P. L.; Baglioni, P. Molecular Recognition in Supramolecular Structures Formed by Phosphatidylnucleosides−Based Amphiphiles. *Colloids Surf., A* **2000**, *167*, 95−103.
(35) Wang, Y.; Desbat, B.; Manet, S.; Aimé, C.; Labrot, T.; Oda, R. Aggregation Behaviors of Gemini Nucleotide at the Air−Water Interface and in Solutions Induced by Adenine−Uracil Interaction. *J. Colloid Interface Sci.* **2005**, *283*, 555−564.
(36) Aimé, C.; Manet, S.; Satoh, T.; Ihara, H.; Park, K.; Godde, F.; Oda, R. Self−Assembly of Nucleoamphiphiles: Investigating Nucleosides Effect and the Mechanism of Micrometric Helix Formation. *Langmuir* **2007**, *23*, 12875−12885.
(37) Zana, R.; Levy, H.; Papoutsi, D.; Beinert, G. Micellization of Two Triquaternary Ammonium Surfactants in Aqueous Solution. *Langmuir* **1995**, *11*, 3694−3698.
(38) Dazzazi, A.; Coppel, Y.; In, M.; Chassenieux, C.; Mascalchi, P.; Salome, L.; Bouhaouss, A.; Kahn, M. L.; Gauffre, F. Oligomeric and Polymeric Surfactants for the Transfer of Luminescent ZnO Nanocrystals to Water. *J. Mater. Chem. C* **2013**, *1*, 2158−2165.
(39) In, M.; Bec, V.; Aguerre-Chariol, O.; Zana, R. Quaternary Ammonium Bromide Surfactant Oligomers in Aqueous Solution: Self-Association and Microstructure. *Langmuir* **1999**, *16*, 141−148.
(40) Shimizu, S.; Pires, P. A. R.; El Seoud, O. A. ^{1}H and ^{13}C NMR Study on the Aggregation of (2-Acylaminoethyl) Trimethylammonium Chloride Surfactants in D_2O. *Langmuir* **2003**, *19*, 9645−9652.
(41) Ma, J.-H.; Guo, C.; Tang, Y.-L.; Zhang, H.; Liu, H.-Z. Probing Paeonol−Pluronic Polymer Interactions by 1H NMR Spectroscopy. *J. Phys. Chem. B* **2007**, *111*, 13371−13378.
(42) Kessler, H.; Gehrke, M.; Griesinger, C. Two-Dimensional NMR Spectroscopy: Background and Overview of the Experiments [New Analytical Methods (36)]. *Angew. Chem., Int. Ed.* **1988**, *27*, 490−536.

DOI: 10.1021/acsami.5b04441
ACS Appl. Mater. Interfaces 2015, 7, 15078−15087